Geometric phases in two-photon interference experiments

J. Brendel,[1] W. Dultz,[1,2] and W. Martienssen[1]
[1]*Physikalisches Institut der Universität Frankfurt am Main, 60054 Frankfurt am Main, Germany*
[2]*Forschungs und Technologiezentrum der Deutschen Telekom, 64276 Darmstadt, Germany*
(Received 1 March 1995)

Photon pairs produced by type-I and type-II parametric down-conversion are passed through a Michelson interferometer. Two quarter-wave plates in one arm of the interferometer allow variation of the polarization state of the photons. We investigate experimentally the geometric phase or Pancharatnam phase acquired by single photons and photon pairs dependent on the solid angle that is subtended by the circuit that represents the varying state of polarization on the Poincaré sphere. It is found that the geometric phase acquired by the pair depends on the initial polarization state of the two photons. If both photons are in equal states of linear polarization, we observe a doubling of the geometric phase compared to single photons; in the case of orthogonal states of linear polarization, the geometric phase is completely canceled. Our results show the role of Pancharatnam's phase in nonclassical two-photon interference phenomena and the interplay between the geometric phase and the dynamical phase in these phenomena.

PACS number(s): 03.65.Bz, 42.50.Dv

I. INTRODUCTION

Starting from Berry's studies of the *quantal phase factors accompanying adiabatic changes* [1], a lot of work has been done to observe this geometric phase change in the state of a quantum system whose environmental parameters are slowly changed. Geometric phases appear in various physical systems (for a review, see, e.g., [2]). In optics, the attention has been drawn to a much earlier paper by Pancharatnam [3]. In his paper Pancharatnam discusses the phase shift that takes place in light fields if one changes the state of polarization. Pancharatnam's phase can be regarded as the manifestation of Berry's phase in polarization optics. This important connection has been widely discussed (see. e.g., [4]). Since it offers the possibility of rather simple experimental approaches, geometric phases in optics have been subject to several experimental and theoretical investigations.

Until now, geometric phases in optics have only been observed in experiments with classical light fields [5–10] and with single photons [11,12]. In both cases a classical, as well as a quantum treatment predict the same geometric phase shift, since the phase is measured via the mutual coherence function [6]. As shown by Klyshko [13], a light field with n identically polarized photons per mode is expected to acquire n times the phase of a one-photon field, which equals n times the phase of a classical field. For arbitrary polarized photons this equivalence between the geometric phase of a quantum multiphoton field and of a classical field is no longer valid.

Regarding pairs of identically polarized photons, one expects a doubling of the geometric phase compared to single-photon experiments. In our experiments this particular geometric phase is measured by making a photon pair interfere with itself inside a Michelson interferometer [14]. Hence, the geometric phase introduced by a suitable arrangement of quarter-wave plates in one arm of the interferometer shows up as a shift of the two-photon interference pattern. In addition we demonstrate that, depending on the relative orientation of the vectors representing the states of polarization of the photons of a pair, a cancellation of the geometric phase is also possible. Furthermore, our results will give some insight into the interplay between the geometric phase and the dynamical phase in two-photon interference phenomena.

II. EXPERIMENTAL SETUP

Our experimental setup is shown in Fig. 1. The photon pairs are generated in a beta barium borate (BBO) crystal by down-conversion of the blue light ($\lambda = 458$ nm) from an Argon laser, which provides an optical output power of about 100 mW. Using an intracavity etalon, we reduce the bandwidth of the laser light to 54 MHz and achieve a coherence length of about 5 m. Only photon pairs emitted colinear with the laser beam are selected by the aperture A. The central wavelength of the two-photon light is 916 nm, and its spec-

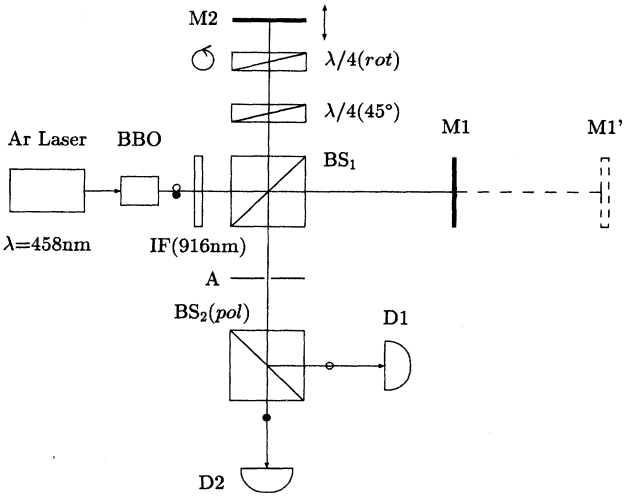

FIG. 1. Outline of the experimental setups for the zero path difference ($M1$) and the large-path-difference (dashed lines, $M1'$) case.

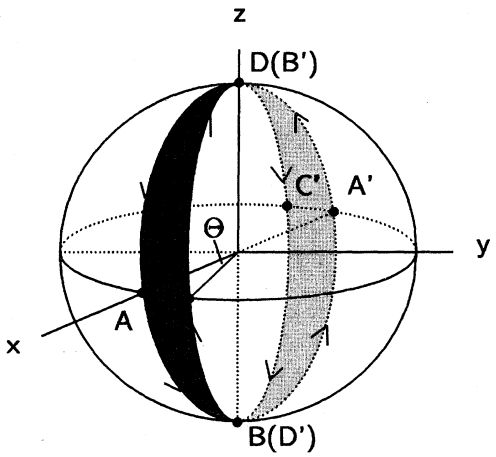

FIG. 2. Representation of the polarization transformations introduced by the quarter-wave plates on the Poincaré sphere. Two circuits for horizontally (solid lines with arrows, starting from point A) and vertically polarized light (dashed lines with arrows starting from point A') are shown.

tral bandwidth is restricted by the interference filter (IF) to 10 nm. By alternatively using two BBO crystals cut for type-I and type-II phase matching, we are able to prepare the photons of a pair in either the same state of polarization (type I) or in orthogonal states of polarization (type II). These pairs traverse the Michelson interferometer consisting of the beamsplitter (BS), which exhibits nearly equal reflection and transmission coefficients for all states of polarization, and the two silver-mirrors $M1$ and $M2$.

After the emergent light has passed the aperture A, the photon pairs are split by the second beamsplitter BS_2 and are then directed to the photon counting avalanche diodes $D1$, $D2$ (RCA SPCM-200). In case of type I phase matching BS_2 is a standard 50/50 beamsplitter. Therefore only one half of the arriving pairs are split. In case of type II phase matching this beamsplitter is replaced by a polarizing beamsplitter BS_2(pol). Now, all of the photon pairs are split and detector $D1$ registers only vertically polarized photons, whereas detector $D2$ registers the horizontally polarized part of the pairs.

The geometric phases are introduced the same way as in previous experiments based on laser-light or single photons [7,6,11] by the help of two quarter-wave plates placed in one arm of the interferometer. The action of these mica plates on the initially horizontally (vertically) polarized light can be conveniently represented by circuits on the Poincaré sphere, as sketched in Fig. 2. The fast axis of the first quarter-wave plate makes a fixed angle of $+45°$ with respect to the horizontal axis. Thus, the polarization states are changed from linear (horizontal or vertical), represented by the points A (A') on the Poincaré sphere, to right (left) circular, represented by the points B (B'). The first passage through the second, the rotatable quarter-wave plate $\lambda/4$(rot) changes the circular polarization back to a linear polarization state C (C'). The resulting polarization vector makes an angle ϕ with respect to the initial vector, where $135°+\phi$ is the orientation of the second quarter-wave plate with respect to the horizontal axis. The projection on the Poincaré sphere gives an azimuthal angle from A to C (A' to C') of $\Theta=2\phi$. After reflection at mirror $M2$, the rotatable retardation plate turns the linear polarization into left (right) circular polarization D (D'). The fixed plate then restores the initial states of polarization.

Hence, for both of the initial linear states of polarization we have a cyclic evolution along the paths $ABCDA$ and $A'B'C'D'A'$, respectively. The solid angle subtended by these circuits, as indicated by the shaded regions, is $\Omega=\pm 4\phi$, where the sign depends on the sense of description. The Pancharatnam phase associated with the circuits is $\delta_p=\frac{1}{2}\sigma\Omega=\pm 2\phi$, where $\sigma=1$ is the spin of the photons.

III. CALCULATION OF THE TWO-PHOTON TRANSMISSION FUNCTIONS

We now turn to the questions, in which way does the two-photon transmission probability P_{22} in a Michelson interferometer depend on the geometric phase δ_p, and how does the geometric phase interact with the dynamical phase. For that we regard the probability amplitudes associated with the different processes that lead to a transmission of the photon pair through the interferometer. We first assume that the interferometer is adjusted to path differences that are much smaller than the coherence length of the light, allowing (classical) second-order interferences of the transmitted beams. The dynamical phases introduced by the path difference between the interfering light fields are symbolized by δ_s and δ_i for the signal and the idler beam, respectively. The geometric phases associated with the circuits on the Poincaré sphere are symbolized by δ_{ps} and δ_{pi}, correspondingly. Summing up the probability amplitudes for the four possible ways the pairs can choose to pass the interferometer [15,16], we obtain, using a single-mode approximation,

$$P_{22}(\delta_s,\delta_i,\delta_{ps},\delta_{pi})=|r^2t^2(1+e^{i(\delta_s+\delta_{ps})}+e^{i(\delta_i+\delta_{pi})}+e^{i(\delta_s+\delta_{ps}+\delta_i+\delta_{pi})})|^2. \quad (1)$$

The values of the Pancharatnam phase for the signal and the idler photons only depend on their initial states of linear polarization. Assuming equal polarization (type-I phase matching), we can simplify Eq. (1) by setting

$$\delta_{ps}=\delta_{pi}=\delta_p, \quad \delta_s=\delta_i=\delta. \quad (2)$$

The second constraint arises from the assumption of frequency degeneracy.

Under these conditions, Eq. (1) yields the two-photon transmission probability

$$P_{22}^I(\delta,\delta_p)=4r^4t^4[1+\cos(\delta+\delta_p)]^2. \quad (3)$$

The probability (3) equals the square of the transmission probability expected for single photons P_{11}, and it is proportional to the square of the classical intensity of the light field: $P_{22}=P_{11}^2\sim I^2$. This result is not surprising when we consider the measurement of intensity correlations or the joint transmission probability of independent photons.

As shown above, the signs of the Pancharatnam phase for orthogonally polarized photons are opposite ($\delta_{ps}=-\delta_{pi}$

$=\delta_p$). Therefore the probability amplitudes for the transmission of pairs created by degenerate type-II phase matching add up to

$$P_{22}^{\mathrm{II}}(\delta,\delta_p)=4r^4t^4[1+\cos(\delta+\delta_p)+\cos(\delta-\delta_p)+\tfrac{1}{2}\cos(2\delta)+\tfrac{1}{2}\cos(2\delta_p)]$$
$$=4r^4t^4[1+\cos(\delta+\delta_p)][1+\cos(\delta-\delta_p)]. \quad (4)$$

Again, the joint transmission probability is given by the product of the probabilities for the single signal and idler photons.

In both cases discussed above, we could not discriminate between the different photon pair transmission processes through the interferometer. There are two processes where we may picture the photon pairs as being split when entering the interferometer. For these processes the geometric phase is brought in for the single photons passing the arm which contains the quarter wave plates. Therefore, in order to investigate the geometric phase shift arising from the passage of a photon pair through the quarter wave plates, these single photon processes have to be excluded from registration. As we have demonstrated in previous publications [14,17], this can be done experimentally by increasing the path-difference Δx between the interferometer arms. That way, the split photons reach the output with a relative time delay of $\Delta x/c$. If this delay exceeds the maximum time difference accepted for coincidence detection, these processes will not be registered as coincidences and the interference of the photon-pair with itself can be observed alone.

In contrast to classical (second-order) interference this fourth-order interference is still possible even if the path difference exceeds the coherence length of the two-photon light by far. The maximum path difference allowing interference is only restricted by the coherence length of the pump laser. Keeping the path difference far below the coherence length of the laser, phase fluctuations due to incoherence can be neglected and the interference can again be described by a simplifying single-mode treatment. Adding the probability amplitudes as above, now for the two remaining processes alone, yields

$$P_{22}(\delta_s,\delta_i)=|r^2t^2(1+e^{i(\delta_s+\delta_i+\delta_{ps}+\delta_{pi})})|^2. \quad (5)$$

For parallelly polarized photons (degenerate type-I phase-matching) the constraints (2) are valid and Eq. (5) leads to

$$P_{22}(\delta,\delta_p)=2r^4t^4[1+\cos(2\delta+2\delta_p)]. \quad (6)$$

For orthogonally polarized photons (degenerate type-II phase-matching) Eq. (5) leads to

$$P_{22}(\delta,\delta_p)=2r^4t^4[1+\cos(2\delta)]. \quad (7)$$

According to Eqs. (6) and (7) we expect interferograms that correspond to a doubling of the dynamical phase and exhibit visibilities of 1. This nonclassical property of two-photon interference has already been demonstrated in several previous experiments [14,18,19]. The above calculations now also take into account the role of the geometric phase δ_p and its interplay with the dynamical phase δ. Equation (6) verifies the predicted doubling in case of parallelly polarized photons. For orthogonally polarized photons the geometric phase is canceled due to the opposite handedness of the related circuits on the Poincaré sphere.

IV. EXPERIMENTAL PROCEDURES AND RESULTS

A. Experiments at small path differences

Using the experimental setup shown in Fig. 1, we have carried out several experiments to demonstrate the above predicted special properties of the geometric phase in two-photon interference. To begin with, the interferometer is adjusted close to the white light position, i.e., the path difference is kept far below the coherence length of the detected light. We record the counts of the single detectors $D1$ and $D2$, as well as their coincidences in dependence on the geometric phase introduced by the quarter-wave plates and on the dynamical phase associated with the optical path-difference Δx. The counts are registered and stored by personal-computer-based multichannel counters. The quarter-wave plate $\lambda/4$(rot) is rotated in steps of the angle ϕ of 3.6° using a stepping motor that is synchronized with the channel advanced of the counters. The dynamical phase is varied by shifting mirror $M2$ stepwise simultaneously by a piezo translation stage.

Figure 3 shows the single-photon [3(a)] and two-photon [3(b)] interferograms obtained for photon pairs generated by degenerate type I phase matching (both photons are horizontally polarized). The plotted counts have been integrated during time intervals of 2 s for each single detector and during 4 s for the coincidences. To simplify the presentation only the counts of detector $D1$ are displayed in Fig. 3(a). Detector $D2$ delivers almost identical interferograms.

The left interferograms in Figs. 3(a) and 3(b) have been recorded keeping mirror $M2$ at a fixed position, while the quarter-wave plate makes one full counterclockwise turn (looked at from the beamsplitter BS_1). This rotation introduces a maximum geometric phase shift of 2π, as indicated by the lower x axis. In the next step we change the dynamical phase simultaneously with the geometric phase by shifting mirror $M2$ in such a way that the arm length BS_1-MS increases in steps of 15.1 nm, as indicated by the upper x axis. This displacement corresponds to an increase of the path difference Δx by an amount of 30.2 nm, or to an increase of the dynamical phase δ by 11.87°. At the same time the quarter-wave plate is rotated with each step by an angle of 3.6°.

We now obtain interferograms as shown in the middle and, with the sense of rotation reversed (clockwise), on the right. The fully drawn curves are fits to the data by the functions $f_1(\phi,\delta)=\alpha[1+V_0\cos(2\phi+\delta+\delta_0)]$ for the single counts and by $f_2(\phi,\delta)=\beta f_1(\phi,\delta)^2$ for the coincidences, respectively [see Eq. (3), assuming $\delta_p=2\phi$]. Here, α and β are scaling parameters and the initial phase δ_0 has been set to $-\pi/2$ by an appropriate choice of the presented data range. Good fits are obtained using visibility factors V_0 of 0.86 for the interferograms on the left and in the middle and of 0.88 for those on the right.

Figure 4 shows equivalent interferograms, recorded after the experimental setup has been changed to the type-II down-conversion configuration. The quarter-wave plate is

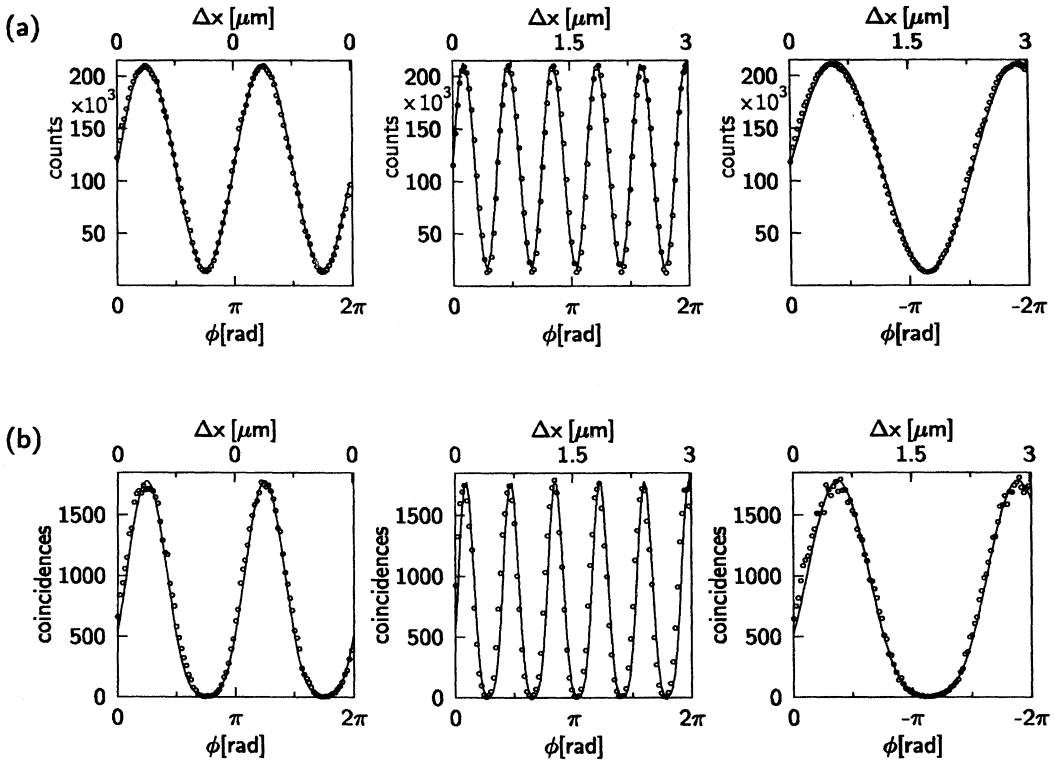

FIG. 3. Measured second-order (a) and fourth-order (b) interferograms using type-I phase matching. The interferograms in the first column show the geometric phase introduced by rotating the quarter-wave plate alone; for those in the second and third column a dynamical phase shift has been added by shifting mirror $M2$ simultaneously. The third column differs from the second by a reversed direction of rotation. The rotation angle ϕ of the quarter-wave plate $\lambda/4$(rot) is represented by the lower x axis, and the path difference Δx that is introduced by shifting mirror $M2$ by the upper x axis.

again rotated counterclockwise by steps of 3.6°, while the path length is increased by steps of 30.2 nm. The counts of detector $D1$, which now registers only the vertically polarized photons, are represented by circles; the counts of detector $D2$, which registers the horizontally polarized photons, are represented by filled triangles. The single-photon data are again fitted by functions $f_1, f_{1'}$ (fully drawn lines) as above with visibility factors of $V_0 = 0.86$. Due to the orthogonal polarization states these functions now differ by opposite signs for the geometric part of the phase [see Eq. (4)]. The lower graph displays the simultaneously recorded coincidences. The fully drawn line is again a fit to the data by the product of the single-photon functions $\beta f_1 f_{1'}$.

B. Experiments at large path differences

In the following section we present the results obtained after increasing the distance BS_1-$M1$ from 100 to 250 mm. The photons passing this arm now suffer a delay of 1 ns compared to those in the other arm. Reducing the width of the coincidence window to 0.5 ns we detect only photon pairs that traverse the interferometer without being split. The geometric phases gained by those pairs which pass the quarter-wave plates are shown in Figs. 5 and 6. Care has been taken to keep the dynamical phase constant by a stable experimental setup and a constant room temperature.

Figures 5 and 6 are plots of the coincidences obtained when the quarter-wave plate is turned clockwise by 360° in steps of 1.8°. The counts are integrated over 10 s at each position of the stepping motor. The interferogram shown in Fig. 5 has been recorded using type-I phase matching. The fully drawn line is a fit to the experimental data by the function $f(\phi) = \alpha[1 + V_0 \cos(4\phi + \delta_0)]$ [see Eq. (6)]. A least-mean-square fit yields a visibility of $V_0 = 0.78$. The single detectors exhibit constant count rates of 18 and 13 kHz, respectively.

The results shown in Fig. 6 have been recorded after changing the experiment to the type II down-conversion setup. The fully drawn line is a fit to the data by the function $f(\phi) = \text{const}$ [see Eq. (7)]. The count rates of the single detectors are again constant (5, 4 kHz). To ensure that the observed vanishing of the interference is not caused by a misalignment of the apparatus, we have performed a similar measurement, now introducing a dynamical phase by scanning mirror $M2$. This measurement revealed interferences with a visibility of about 0.78.

Due to the low rate of dark counts ($\approx 50\ \text{s}^{-1}$) and the small coincidence windows (2, 0.5 ns) no correction of all presented data has been made for dark counts or accidental coincidences.

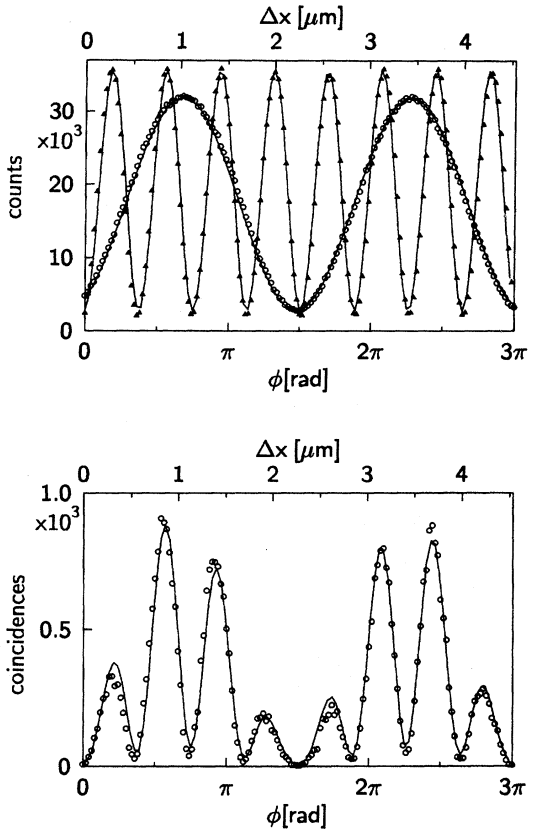

FIG. 4. Measured second-order (above) and fourth-order (below) interferograms presented as in Fig. 3, now using type-II phase matching. The dynamical and Pancharatnam's phase have been altered simultaneously.

V. DISCUSSION AND CONCLUSIONS

Our results presented above show the specific properties of the geometric phase in two characteristic cases of two-photon interference. First, in case of an interferometer adjusted to a path difference far below the coherence length of the light, second-order (single-photon) interferences are still observed. For these interferences the roles of the dynamical phase and the geometric phase are equivalent; they simply add. In this case the observed fourth-order (two-photon) interferograms are given by the product of the single-photon interferograms, as shown in Figs. 3 and 4. There is a simple explication for this behavior if we assume that the photons of each pair pass the interferometer independently. The assumption of independence seems to be in contrast to the fact that the photons are initially prepared in a quantum state consisting of two photons that are highly correlated in energy and time. Regarding Eqs. (1)–(4) we find that the interference of the quantum-mechanical probability amplitudes here yields the same result as expected for independent photons. This implies that the role of the geometric phase can also be understood classically if we consider the phase shift in a corresponding measurement of intensity correlations. Similar results have previously been found in experiments dealing with the dynamical phase [15].

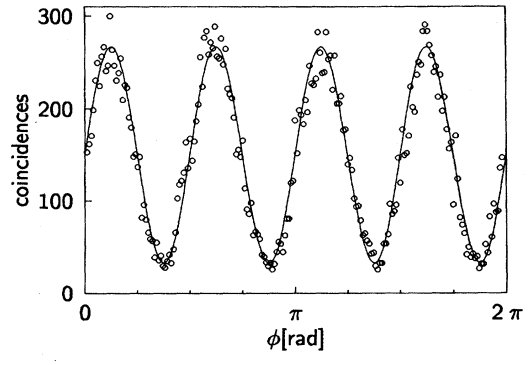

FIG. 5. Fourth-order interferences in the large-path-difference interferometer showing Pancharatnam's phase dependency on the rotation angle ϕ of the second quarter-wave plate $\lambda/4$(rot). The photons of the pairs are parallelly polarized (type-I phase matching).

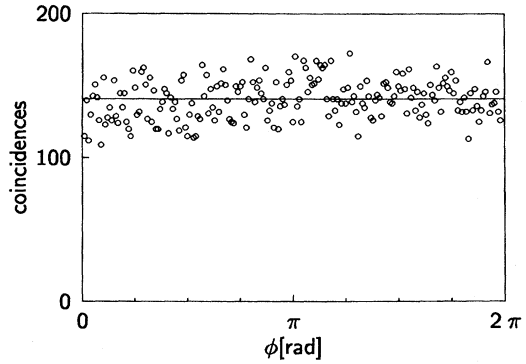

FIG. 6. Fourth-order interferences in the large-path-difference interferometer, as in Fig. 5, showing Pancharatnam's phase where the photons of the pairs are orthogonally polarized (type-II phase matching).

These results also explain why, regarding parallelly polarized photons, we cannot distinguish between a dynamical phase introduced by altering the path difference and a geometric phase introduced by the quarter-wave plates. Only if we prepare the photons in different states of polarization (type-II phase matching), a difference between these phases becomes obvious. Then the polarization dependence of the geometric phase leads to a significant change of the correlation interferograms when tuning the dynamical phase or the geometric phase, alternatively. In this case, the phases are no longer additive [see Eq. (4)], since we find opposite signs of the geometric phase for the orthogonal polarization states. This property opens up the possibility of introducing an arbitrary phase difference between photons belonging to orthogonal polarization states by choosing an appropriate orientation of the quarter-wave plate $\lambda/4$(rot).

In contrast to the experiments discussed above the second series of our experiments allows the observation of the geometric phase for a photon pair alone. Now, the single-photon processes are excluded from detection by using large-path-difference interferometers and a time-resolved coincidence detection scheme. A consequence of the remaining quantum two-photon interference is that the photon pair transmission

probability is no longer given by the product of the single-photon probabilities. This result reveals the entanglement of the two-photon state generated by parametric down conversion. Once again, like in several previous experiments, entanglement turns out to be the fundamental basis for the demonstration of local and nonlocal quantum correlations. (For a more detailed discussion of the two-photon entanglement, see, e.g., [20,21]).

As shown in Fig. 5, the recorded correlation interferogram exhibits half the period, as expected from a classical light field. This result implies that the photon pairs gain twice the geometric phase of single photons, or that the pairs seem to behave like single particles possessing a doubled spin of $\sigma=2$. We find an easy explication of this behavior by taking into account that each of the photons of a pair passing the quarter-wave plates acquires a geometric phase of δ_p [see Eq. (5)]. Here again an equivalence to similar experiments based on the dynamical phase [14] becomes obvious. Since the dynamical phase is also gained twice by the photon pair, the two-photon interferograms are equivalent to those expected for single photons of doubled energy.

The geometric phase depends, as shown above, on the polarization state of the photons, whereas the dynamical phase is given by the path difference alone. Therefore the equivalence between tuning the interferometer via the dynamical phase or the geometric phase will not be valid when passing photons of different polarization states through the interferometer. As an extreme, orthogonally polarized photons acquire geometric phases of opposite signs. If we consider a photon pair composed of two orthogonally polarized photons as one quasiparticle, then this *two photon* is not influenced by the geometric phase at all; it behaves like one particle with total spin $\sigma=0$. This property is demonstrated by the vanishing of the interference, as shown in Fig. 6.

The fact that the orthogonally polarized single photons of the pairs actually acquire a geometric phase can be demonstrated by sending each of them in one of two separated, identical interferometers. This setup allows the observation of nonlocal two-photon interferences and has previously been used to demonstrate violation of Bell's inequality for energy and time [17,22]. The work presented here shows that also in quantum single- and two-photon interference experiments the tuning of the interferometers can be carried out using geometric phases. Provided that the dynamical phases are kept constant, this method offers several advantages. First, the phase tuning can simply be accomplished by rotating a wave plate, and thus definite reproducible settings of the phase differences are easily possible. Due to the wavelength independence of the geometric phase, these settings can, in principle, also be established for broadband light fields. These properties offer applications in tests of Bell's inequality and in quantum cryptography schemes.

Our results cannot solve the frequently discussed question of whether geometric phases in optics have a quantum or a classical origin [23]. The answer depends on the individual approach to the problem. But we have demonstrated quantum-optical two-photon interferences based on the geometric phase. It becomes evident that geometric phases in nonclassical interference phenomena play an important role, just like they do in classical interference, and that practical applications are straightforward.

ACKNOWLEDGMENTS

The authors thank Professor E. Mohler for many stimulating discussions. This work is supported by the Deutsche Telekom.

[1] M. V. Berry, Proc. R. Soc. London A **392**, 45 (1984).
[2] *Geometric Phases in Physics*, edited by A. Shapere and F. Wilzek (World Scientific, Singapore, 1989).
[3] S. Pancharatnam, *Collected Works of S. Pancharatnam* (Oxford University Press, London, 1975).
[4] M. V. Berry, J. Mod. Opt. **34**, 1401 (1987).
[5] A. Tomita and R. Y. Chiao, Phys. Rev. Lett. **57**, 937 (1986).
[6] R. Simon, H. J. Kimble, and E. C. G. Sudarshan, Phys. Rev. Lett. **61**, 19 (1988).
[7] T. H. Chyba, L. J. Wang, L. Mandel, and R. Simon, Opt. Lett. **13**, 562 (1988).
[8] R. Bhandari and J. Samuel, Phys. Rev. Lett. **60**, 1211 (1988).
[9] R. Y. Chiao *et al.,* Phys. Rev. Lett. **60**, 1214 (1988).
[10] H. Jiao, S. R. Wilkinson, and R. Y. Chiao, Phys. Rev. A **39**, 3475 (1989).
[11] P. G. Kwait and R. Y. Chiao, Phys. Rev. Lett. **66**, 588 (1991).
[12] T. P. Grayson, J. R. Torgerson, and G. A. Barbosa, Phys. Rev. A **49**, 626 (1994).
[13] D. N. Klyshko, Phys. Lett. A **140**, 19 (1989).
[14] J. Brendel, E. Mohler, and W. Martienssen, Phys. Rev. Lett. **66**, 1142 (1991).
[15] E. Mohler, J. Brendel, R. Lange, and W. Martienssen, Europhys. Lett. **8**, 511 (1989).
[16] J. Brendel, R. Lange, E. Mohler, and W. Martienssen, Ann. Phys. **7**, 26 (1991).
[17] J. Brendel, E. Mohler, and W. Martienssen, Europhys. Lett. **20**, 575 (1992).
[18] Z. Y. Ou, X. Y. Zou, L. J. Wang, and L. Mandel, Phys. Rev. Lett. **65**, 321 (1990).
[19] P. G. Kwiat *et al.,* Phys. Rev. A **41**, 2910 (1990).
[20] M. H. Rubin and Y. H. Shih, Phys. Rev. A **45**, 8138 (1992).
[21] Y. H. Shih *et al.,* Phys. Rev. A **50**, 23 (1994).
[22] P. G. Kwiat, A. M. Steinberg, and R. Y. Chiao, Phys. Rev. A **47**, R2472 (1993).
[23] S. C. Tiwari, J. Mod. Opt. **39**, 1097 (1992).